N94-36173

NEW DATA SUPPORTING A $^{146,147}Sm$-$^{142,143}Nd$ FORMATION INTERVAL FOR THE LUNAR MANTLE. L.E. Nyquist, NASA Johnson Space Center, Houston, TX 77058; H. Wiesmann, B.M. Bansal, and C.-Y. Shih, Lockheed Engineering and Science Co., 2400 NASA Road 1, Houston, TX 77258.

Table 1. Isotopic abundance of ^{142}Nd in ϵ-units relative to $^{142}Nd/^{144}Nd$ in the Ames standard; normalized to $^{146}Nd/^{144}Nd$ and $^{148}Nd/^{144}Nd$.

Sample	N	ϵ^{142}_{Nd}	
		146 Norm.	148 Norm.
14310	2	−0.11±0.16	−0.40±0.19
14310	6	−0.16±0.07	−0.12±0.11
14310	5	−0.18±0.15	−0.20±0.17
14078	4	−0.12±0.20	−0.16±0.18
14078	5	−0.07±0.12	−0.14±0.16
15076	4	−0.16±0.18	−0.16±0.26
15076	4	−0.19±0.09	−0.27±0.16
15555	1	−0.24±0.54	+0.18±0.21
15555	3	+0.18±0.18	+0.22±0.17
15555	3	−0.07±0.11	−0.17±0.12
74255	1	−0.03±0.22	+0.04±0.26
74255	6	+0.17±0.11	+0.16±0.15
Asuka 31	2	+0.32±0.16	+0.26±0.21
G2	3	−0.07±0.21	+0.08±0.30
BCR−1	2	−0.06±0.26	+0.03±0.30
ORB 1154	3	+0.04±0.21	+0.04±0.30

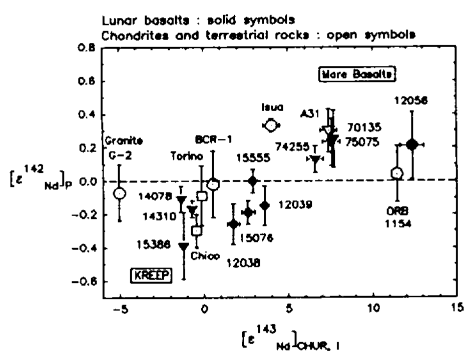

Figure 1. ϵ^{142}_{Nd} for lunar basalts, terrestrial rock standards, the Chico and Torino chondrites, and an Isua supracrustal rock [3].

Abstract: Very small variations in ^{142}Nd abundance in SNC meteorites [1] lunar basalts [1,2] and a terrestrial supracrustal rock [3] have been attributed to the decay of 103 Ma ^{146}Sm initially present in basalt source regions in varying abundances as a result of planetary differentiation. We previously interpreted variations in ^{142}Nd abundances in two Apollo 17 high-Ti basalts, three Apollo 12 low-Ti basalts, and two KREEP basalts as defining an isochron giving a formation interval of ~94 Ma for the lunar mantle [2]. Here we report new data for a third Apollo 17 high-Ti basalt, two Apollo 15 low-Ti basalts, the VLT basaltic lunar meteorite A881757 (formerly Asuka 31), basalt-like KREEP impact melt rocks 14310 and 14078, and three terrestrial rock standards. Those lunar samples which were not exposed to large lunar surface thermal neutron fluences yield a revised mantle formation interval of 237±64 Ma.

Data: Numerical data are reported in Table 1. Quoted error limits are the greater of the standard deviation of the mean ($2\sigma_m$) for N sample analyses, or $2\sigma_p/N^{1/2}$, where σ_p is the standard deviation of a much larger population of standards analyzed in the same sample series. The data were normalized to both $^{146}Nd/^{144}Nd$ and $^{148}Nd/^{144}Nd$ to avoid biases from interferences under the normalization isotope. Typical values of $2\sigma_p$ were $\pm0.16\epsilon$ and $\pm0.18\epsilon$ for $^{142}Nd/^{144}Nd$ normalized to $^{146}Nd/^{144}Nd$ and $^{148}Nd/^{144}Nd$, respectively. Corrections were made for interferences from ^{142}Ce and ^{144,148}Sm using the well-known isotopic compositions of these elements in terrestrial samples. The uncertainties in these corrections are small because the interferences are measured continuously and simultaneously with the isotopes of interest. Additionally, the mass spectrum below and above Nd was scanned at high sensitivity (electron multiplier) prior to data acquisition. The 74255 sample was twice passed through the ion exchange column to remove Ce and Sm from Nd, yielding $^{140}Ce/^{144}Nd$ ~7×10^{-6} ($^{142}Ce/^{144}Nd$ ~1×10^{-6}) and $^{154}Sm/^{148}Nd$ ~2×10^{-5} ($^{144}Sm/^{144}Nd$ ~7×10^{-7}).

Discussion: Figure 1 compares the new data to earlier measurements for lunar basalts and three terrestrial rock standards, USGS standard granite G-2, USGS standard basalt BCR-1, and ocean ridge basalt ORB-1154 [4]. Weighted averages of ϵ^{142}_{Nd} calculated with the two normalizations (Table 1) are plotted as present-day $[\epsilon^{142}_{Nd}]_p$ vs. initial $[\epsilon^{143}_{Nd}]_{CHUR,I}$ relative to a **C**hondritic **U**niform **R**eservoir (CHUR, [5]) at the time of basalt crystallization. The new analyses of 14078 are preferred to those reported previously [2] because of improved instrument and run conditions. A positive correlation is evident for the lunar data, but not for the terrestrial rock standards, for which $^{142}Nd/^{144}Nd$ values are indistinguishable from the Ames shelf standard.

Figure 2 shows some possible evolutionary paths for source reservoirs formed at Δt = 100, 200, and 300 Ma after the angrite LEW86010 [6,7] for "Highly **D**epleted **M**antle" (HDM), "Less

LUNAR MANTLE FORMATION INTERVAL: Nyquist L.E., et al.

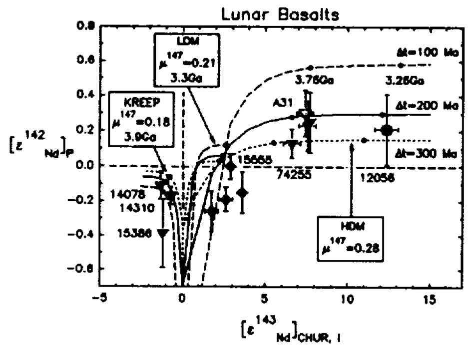

Figure 2. Evolutionary paths from $\epsilon^{142}_{Nd} = -2.69$ at 4.558 Ga ago for the Ames standard and $[^{147}Sm/^{144}Nd]_{CHUR} = 0.1967$.

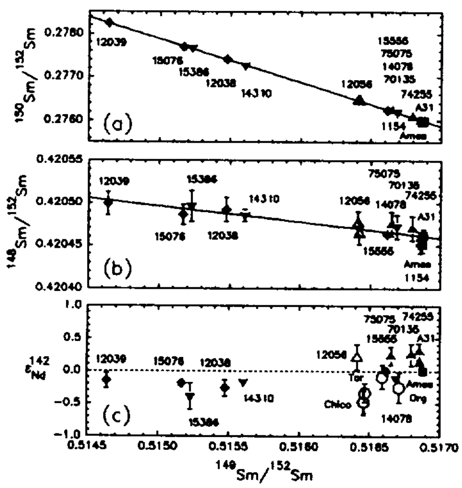

Figure 3. Correlation of (a) $^{150}Sm/^{152}Sm$ and (b) $^{148}Sm/^{152}Sm$ to $^{149}Sm/^{152}Sm$. ϵ^{142}_{Nd} vs. $^{149}Sm/^{152}Sm$ is shown in (c).

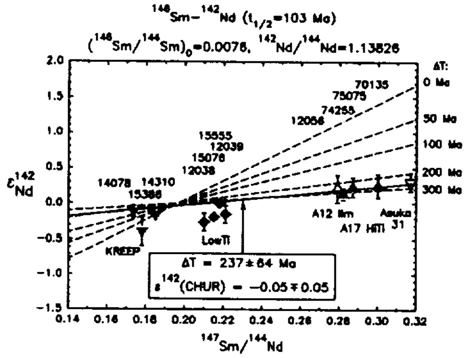

Figure 4. Lunar mantle isochron (see [2]) with updated data. Regression omits samples with high neutron fluence.

Depleted Mantle" (LDM) and the source of lunar KREEP. Values of μ^{147} ($^{147}Sm/^{144}Nd$) assumed for the KREEP, LDM, and HDM sources were 0.18, 0.21, and 0.28, respectively. The evolutionary paths were calculated with the assumptions that $^{142}Nd/^{144}Nd$ of our Ames shelf standard is appropriate for the CHUR-reservoir, which in turn is appropriate to the nascent moon. Neither assumption need be true. Points along the curve show values at basalt ages of 3.9 Ga (KREEP), 3.76 Ga (Apollo 17 high-Ti, Asuka 31 [8]), 3.3 Ga (Apollo 15 low-Ti), and 3.26 Ga (Apollo 12 ilmenite basalt 12056), respectively. The calculated curves provide a reasonable match to the data with the exception of three low-Ti basalts (12038, 15076, 12039) and an earlier analysis of KREEP basalt 15386, which plot below the curves. Nevertheless, the calculations provide at least a qualitative explanation of the rough correlation between $[\epsilon^{142}_{Nd}]_p$ and $[\epsilon^{143}_{Nd}]_{CHUR,I}$ for the lunar basalt data, and for the decoupling of these parameters with decreasing basalt age.

Discussion: Because of uncertainty in the lunar initial ϵ^{142}_{Nd}, we developed the lunar mantle isochron approach which is based on lunar ^{146}Sm-^{142}Nd systematics alone [2]. However, the possibility of non-radiogenic contributions to the variations in lunar $^{142}Nd/^{144}Nd$ ratios also must be considered. Cosmic-ray induced variations in the relative abundances of ^{149}Sm and ^{150}Sm due to thermal neutron capture by ^{149}Sm provide a sensitive monitor of lunar surface irradiation (Figure 3a). The Sm isotopic data for these samples also suggests neutron-induced variations of up to ~1 ϵ-unit in the abundance of ^{148}Sm, in spite of a thermal neutron capture cross section for ^{147}Sm which is nearly 1000-fold less than that of ^{149}Sm (Figure 3b). The thermal neutron capture cross section for ^{142}Nd is ~three-fold lower still, and no trend of ϵ^{142}_{Nd} with $^{149}Sm/^{152}Sm$ is clearly established. Nevertheless, there is a tendency among basalts of a given type for those with high neutron fluences to have low ϵ^{142}_{Nd} (12038, 12039 and 15076 vs. 15555; 15386 and 14310 vs. 14078). Omitting samples with high neutron fluence from the lunar mantle isochron regression (Figure 4) yields $\Delta t = 237 \pm 64$ Ma and $[\epsilon^{142}_{Nd}]_{CHUR} = -0.05 \pm 0.05$ (2σ from the Williamson [9] regression). These parameters differ from $\Delta t = 94 \pm 23$ Ma, $[\epsilon^{142}_{Nd}]_{CHUR} = -0.31$ found previously [2] primarily because of revised data for 14078 and exclusion of samples with high neutron fluence. Disregarding uncertainties in initial $[\epsilon^{142}_{Nd}]_{CHUR}$, both Figures 2 and 4 show that the HDM must have formed substantially (~100-300 Ma) after ancient meteorites such as the angrites in order not to have easily observed enhancements in ϵ^{142}_{Nd} in basalts derived from it.

REFERENCES: [1] Nyquist L.E. et al. (1991) Meteoritics 26, 381. [2] Nyquist L.E. (1993) LPS XXIV, 1095-1096. [3] Harper C.L., Jr. and Jacobsen S.B. (1992) Nature 360, 728-732. [4] Kay R. et al. (1970) JGR 75, 1585-1613. [5] DePaolo D. J. and Wasserburg G.J. (1976) GRL 3, 249-252. [6] Nyquist L.E. (1991) LPS XXII, 989-990. [7] Lugmair G.W. and Galer S.J.G. (1992) GCA 56, 1673-1694. [8] Misawa K. et al. (1993) GCA 57, 4687-4702. [9] Williamson J.H. (1968) Can. J. Phys. 46, 1845-1847.